GloveSignature: A Virtual-Reality Based System for Dynamic Signature Verification

توقيع قفاز البيانات: نظام يعتمد على الواقع الإفتراضى للتحقق من صحة التوقيع بطريقة ديناميكية

A.S. Tolba

Electrical Eng. Dept., Suez-Canal University, Port-Said

ملخص البحث.

يقدم البحث طريقة جديدة تعتمد على استخدام قفاز البيانات للتعرف على التوقيع والتحقق من صحته وذلك بتسجيل البيانات الخاصة بزوايا انحناء الأصابع ودوران رسغ اليد وميل اليد أثناء عملية التوقيع. نظرا لكم حجم هذه البيانات يتم تركيزها فى عدد محدود من السمات التى تمثل البيانات بدرجة عالية من الدقة وتحافظ على المعلومات بها وذلك باستخدام طريقة تحليل المركبات الأساسية . تستخدم السمات المستخلصة من صيغ إشارات رقمية فى تدريب شبكة عصبية اصطناعية ذاتية التنظيم لتصنيف التوقيع والتحقق من صحته

Abstract

A survey of the principal schemes in the literature suggested that a new way of addressing the problem of signature recognition be formulated in order to find a satisfactory solution for eliminating random forgeries. A fundamental problem in the field of off-line signature recognition is the lack of a pertinent shape representation or shape factor. This paper introduces a novel idea for a dynamic signature recognition system. An initial attempt is presented to demonstrate the data glove as an effective high-bandwidth data entry device for signature recognition. GloveSignature is a virtual reality based environment to support the signing process. The proposed approach retains the power to discriminate against forgeries. This paper extends the use of instrumented data gloves - gloves equipped with sensors for detecting finger bend, hand position and orientation for recognizing hand signatures. Several researchers have already explored the use of gloves in other application areas but using the gloves for the recognition of hand signatures is never reported. An attempt is made in this research to explore the feasibility of using the 5th Glove in on-line signature recognition. Two hundred signatures were collected from twenty subjects, and features were extracted. We demonstrate the effectiveness of a hybrid technique which is based on both the most discriminating eigenfeatures and self-organizing maps (SOFMs) for signature recognition.

Index Terms – Virtual reality, on-line signature recognition, principal component analysis, eigen signatures, feature selection, self-organizing maps, signature recognition, data gloves.

1. Introduction

Having a reliable method to prevent unauthorized transaction or disclosure is essential in the use of computers for business transactions or for access of proprietary data. The problems with current systems such as keyboards or special input terminals such as remembering the various passwords, or Personal Identification Numbers (PINs), keeping them secret and keying them inaccurately render them unreliable. On-line signature verification with data gloves solves most of these problems and makes the forging impossible.

In this paper, we outline a new approach for signature recognition that is secure to skilled forgery (see section 4). Hand gloves provide data on both the dynamics of the pen motion during the signature and the individual's hand shape. Signature verification using the dynamic signature data results in much simpler and faster approach than the most widely used image analysis approaches. Significant in this regard is that skilled forgers cannot reproduce the movement dynamics that occur with an authentic signature. Another point is that hand size is considered while using the data glove.

Accepted August 16, 1999

Static hand posture recognition is currently the most common and widely used method for interaction using glove input devices. In this paper we explore the use of data gloves in the field of hand signature recognition.

Dynamic Signature Recognition (DSR) is difficult for various reasons. The large variations in the speed of execution of various phases of a signature is one such reason. Another reason is the quality and positions of the physical properties describing the signature themselves. These problems are then exaggerated by the differences which arise when the same person attempts repeated executions of the same signature. Other factors effecting the difficulty of DSR are the emotional state of the signing person and the accuracy of the input device used. And finally, a large amount of data has to be processed in real time because of large variances in the length of time to execute a signature. In this paper we describe our approach to overcoming the difficulties of DSR using neural networks. Self-organizing maps have already proven themselves to be appropriate and efficient for signature recognition [1]. However, the extensive amount of data involved in DSR requires a different approach. Because of features such as topology preservation and automatic learning, Kohonen's Self-Organizing Feature Maps (SOFM) are particularly suitable for the reduction of the high dimensional data space which is the result of a dynamic signature, and are thus implemented for this task.

Virtual hand signatures are on-line recordings of hand movements that are used to verify the identity of a person in banks. We are developing a computerized signature recognition system for both the normal and the blind. The system will provide a new tool for signature verification. Figure 1 shows the components of the proposed system: data acquisition, data reduction using SOFM or principal components analysis (PCA) and collective classification. Virtual hand-signatures are acquired during the period of signing on a paper using the 5th Glove. The acquired signature is processed for data reduction and then classified in the recognition stage.

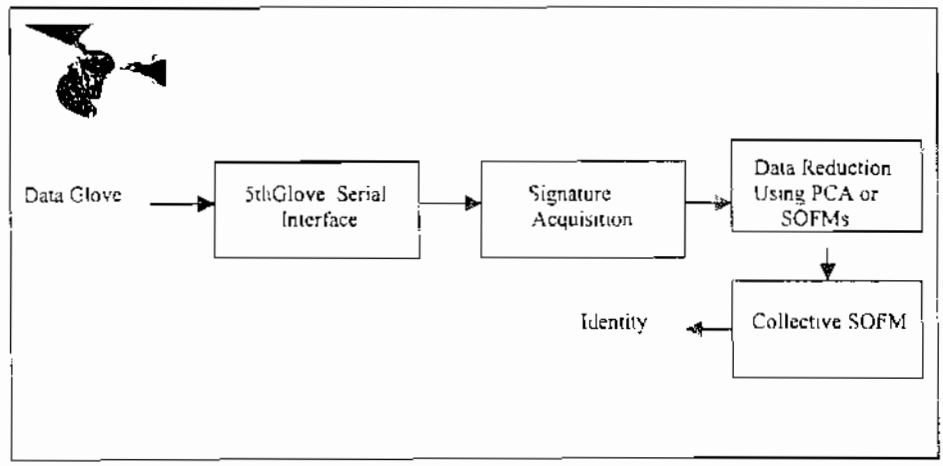

Figure 1: Virtual-Signature Recognition System

In section 2 we present a detailed review of the previous work in the field of signature verification. In section 3, we describe the dynamic signature-data acquisition process and some issues related to the nature of the acquired data. The system architecture is described in section 4. Feature extraction and dimensionality reduction using both the self-organizing feature maps and the principal component analysis are discussed in section 5. In section 6, the neural network classifier is described. In section 7, experimental results and discussion are provided. Section 8 concludes the paper

2. Overview of Previous Work in Signature Verification

In this section, we will discuss some of the more prominent research efforts made in the area of signature recognition. Detailed surveys can be found in [2-4]. Within the last years a wide variety of feature extraction and classification methods have been applied to the signature recognition. While much progress has been made toward signature verification, reliable techniques for signature verification in the case of skilled forgeries have proven elusive. Signature verification approaches are commonly categorized into three major categories, the image-based (static/off-line) approaches, the device-based (dynamic/on-line) approaches and the hybrid approaches. We will consider the three approaches separately.

2.1 Image-based (off-line) Approaches to Signature Recognition

Off-line signature recognition is still an open problem. Several approaches have been proposed in the context of off-line signature verification, like two-dimensional transforms, histograms of directional data, horizontal and vertical projections of the writing trace of the signature, structural approaches, local measurements made on the trace of the signature and the position of feature points located on the skeleton.

In [1], a new approach is described for checking the consistency of biometric databases, and a special application on signature recognition is given. A neural network based consistency measure is proposed to quantify the intra-variability of the individual's signatures. A variance based measure is computed from the output of a trained 2D-self organizing map to check the consistency of the signatures of the same writer. This measure has two purposes: the user can be asked to sign again if the inconsistency degree is higher than a pre selected threshold level, and the avoidance of human error when building a training set by detecting outliers. Having achieved both goals, signature recognition procedures can be implemented.

A democratic neural network architecture is presented for minimization of the reject error rate and maximization of the correct classification based on well-known feature sets and a new feature set. The used signature database consisted of a training set including 100 signatures acquired from 10 subjects and a test set including 60 other signatures acquired from 6 randomly selected subjects from the ten signers. Signatures were recorded over multiple sessions to intentionally encompass the intra-personal variations. The signatures are first thresholded. The minimum bounding rectangle of each signature is then specified. The following four different feature groups are extracted:

1- The first seven moment invariants of the whole signature,
2- A set of association features including the entropy of the signature when considered as a contingency table, and the linear correlation coefficient between the vertical and horizontal projections
3- Statistical features such as the skewness, the kurtosis, and the coefficient of variation extracted from the concatenated horizontal and vertical projections.

The False Rejection Rate (FRR) of the individual feature sets when used with three dimensional Self-Organizing map classifier is shown in Table 1.

Table 1. The False Rejection Rates for Individual Feature Sets with Individual Neural Classifiers

Feature Set	FRR
Moment Invariants	17%
Concatenated Horizontal and Vertical Projections	9%
Association Features	11.3%
Statistical Features of Projections	11%

The implementation of a democratic neural network architecture which votes between the outputs of the four self-organizing maps resulted in a 0.0% FAR with 3% rejection.

In [5], a method for off-line signature verification based on geometric feature extraction and neural network classification is described. A total of 3528 signature images is collected to form the signature database. Signatures are acquired using a scanner at resolution of 300 dpi in bit gray-scale. Median and average filtering techniques are used for standard noise reduction. Binarization of signatures is followed by morphological operations to fill small holes and to remove small disconnected components mostly generated by noisy backgrounnd. Geometrical features are simultaneously computed under several scales by a neural network classifier. The following features are selected to form the [illegible] signature: baseline, ink

area distribution, and signature frontiers. A set of directional features is used to segment the signature into constituent parts. Signature shape is learned by neural networks at multiple resolutions. Local shape features are extracted by using a set of multiple resolution grids with fuzzified borders overlaid on top of signature shape representation. A Multi-layer perceptron is selected for signature classification. An individual signal verifier is constructed for each enrolled signature class. Each verifier consists of several simple three-layer perceptrons, one network per feature resolution plus a decision network whose function is to combine the response from the feature networks and produce a final confidence rating. All genuine signatures and all forgery signatures are used as testing data. The average false acceptance rate for each signature class is just below 0.05 for a test set of 3360 samples. Under targeted forgery test, the test size is 24 genuine samples and 144 forgeries, the average correct classification rate is about 90% at no rejection. An overall match rating is generated by combining the outputs at each scale. Experiments on 3000 signatures show 90% correct classification.

In [6], an off-line system that is based on both global features and backpropagation neural networks is described. Three types of features have been used:

- Horizontal and vertical projection moments which provide a stetistical measure of the distribution of the signature pixels, and is relatively insensitive to distortions and style variation,
- upper envelope of the signature component, and
- lower envelope of the signature component.

Signatures are binary acquired with a hand held scanner at a resolution of 200 dpi. A modified median filter is used for noise elimination. A filter mnsk of size 7x7 pixels is used. A normalized representation of the signature image is obtained using the eigenvectors and eigenvalues of the signature distribution. The projection based feature set can only be effective if the signature is properly aligned. This issue is not considered in their paper. Aligning the signature can be achieved by rotation the signature around its major axis before extracting the features. But the most important characteristic of projection moments is their relative insensitivity to distortions due to noise and/or minor style variations. Recognition decisions are made on the basis of each feature vector using three different classifiers. Weights assigned to the output of each classifier are determined by the accuracy and reliability of the classifier.

The used signeture database comprised fifteen samples of genuine signatures collected from each of ten individuals. In addition, 100 random forgeries are used for evaluating the system. Classification networks were trained with five randomly selected samples of genuine signatures of each person. The output layer of the neural net includes a number of neurons equal to the number of persons involved in the experiment. The activation values of the correct output neuron is used as a threshold to implement a reject option for the combining net. Table 2 presents the overall experimental results in terms of false acceptance (type II) or misclassification and false rejection (type I) error rates for the complete sample set. A combined classifier resulted in a substantial reduction of error rate. Weighted individual classifier outputs resulted in a reduced error rate of about 3%.

Table 2 Percentage of errors [6]

Error type	Moment	Upper envelope	Lower envelope	Classifier Combination	
				Equal weight	With learning
Type II	10.73	7.85	12.34	6.5	3.0
Type I	--	--	--	3.33	1.0

In [7], a new formalism for signature representation based on visual perception is proposed. Granulometric size distributions of the signature image have been used for the definition of local shape descriptors in attempt to characterize the amount of signal activity in front of the retina located on the focus of anention grid. An internal morphological shape descriptor called the pecstrum is computed by measuring the results of successive morphological openings of the object by a structuring element that increases in size. A database of 800 genuine signatures acquired from 20 individuals is used for testing the system. Both threshold and nearest neighbor classifiers are used. The nearest neighbor classifier showed a total error rate of 0.02% and the threshold classifier resulted in a 1.0% error rate in the context of random forgeries.

In [8], a neural network approach is proposed for off-line signature verification based on the directional probability density function (PDF). The PDF is used as a global shape factor. A standard signature database of 40 signatures written by 20 individuals, (800) images are used in this study. The training set includes the first 20 signatures of each writer, while the test set includes the last 20 signatures. The best back-propagation network classifier architecture resulted in an error rate of 1.24% and rejection rate of 4.506%.

In [9], a wavelet transform based technique is applied for optimal segmentation of handwritten Chinese signatures. An input signature curve is segmented at the inflection points which are located by detecting the zero-crossing points of the wavelet transform of the input signature. Signatures are acquired using a digitizer and are reconstructed by linear interpolation to include the information about the writing velocity of the signature. A database containing 220 genuine signatures of 20 stable signers is constructed. Each signer writes 11 signatures. Strokes are segmented at its points of inflection to retain the corners of a signature. Experimental results for segmentation of only six signers are presented.

In [10], an off-line human signature verification system is presented in which the slant directions of the signature strokes and those of the envelopes dilated signature image are extracted. A Multi-Layer Perceptron (MLP) is used as a classifier. Preprocessing is done before feature extraction. It eliminates stylistic features and performs size normalization. For signature classification, three types of classifiers are tested (Euclidean distance, Minimum misclassification linear classifier and MLP). The best system performance was given by the MLP classifier achieving an equal error rate of 4.7% (95.3% correct) for skilled forgeries on the average.

In [11], a comparative study is presented for a large number of features (210) previously studied in the literature and a set of 12 significant features is selected for recognition of Arabic handwritten signatures. Statistical measures such as the mean, standard deviation and the spread percentage are used for feature selection. Those features that have spread less than 25% for all persons are selected. Experiments were performed on a database including 144 genuine signatures acquired from 9 subjects. Signatures were scanned at different times. The test set consisted of 72 signatures (9 subjects, 8 samples each) and the training set consisted of the remaining 72 samples. The test results yielded 98.6% recognition rate using a fast backpropagation neural network classifier.

In [12], a system that is based on a neural network approach for off-line signature verification is described. The following geometrical features are used to extract 41 metric, statistical, and morphological features:

1- Height/width ratio,
2- Principal axis orientation,
3- Elongation,
4- Slope,
5- Amount of connected components,
6- Hole and cavity attributes,
7- Point densities on different areas.

The 41 parameters are used as an input vector to a two layer perceptron for all signers. An improved back propagation algorithm is used for training the neural network. A database comprising 912 signatures captured from 48 signers is divided into a training set including 480 signatures and a test set including 432 signatures. The input vector to the classifier is first preprocessed using normalization (in mean and variance) and PCA. Preprocessing improves the system performance from 97.2% to 98.1%. Different classifiers are used in testing the system. The two layer perceptron applied to PCA resluted in the best performance of 98.1% correct classification. The identification error rate is 2.8% when there is no rejection, and is 0.2% when 10% of the signatures are rejected. A good feature of the used neural network is that it is robust against segmentation errors (missing segments) as a result of its generalization capability. Verification experiments used a two layer perceptron for each signer. For learning the network, 10 examples of genuine signatures and 45 forgeries were used. The output of the verification network is yes or no. The experiments resulted in an error rate of 1% when there is no rejection and an error rate of 0.1% when 17% of the signatures are rejected.

In [13], algorithms were developed for extracting global geometrical and local grid features which are combined to build a multi-scale verification function. Signatures were scanned using a 8-bit, 300 dpi resolution. Binary thresholded images are then linearly normalized after size normalization. The following global geometrical features were extracted from signature images:

1- Effective horizontal width of signature image ,
2- Slant,
3- Vertical center-of-gravity,
4- Maximum horizontal projection,
5- Area,
6- Number of signature pixels within each grid cell,
7- Baseline shift of the signature image.

T e following local features were used:
1 Angle of corner,
2 Curvature of an arc, and
3- Intersection between line strokes

Results indicated a lower verification error rate and higher reliability than either of single scale functions (geometric and grid). A database consisting 450 signatures is acquired from 25 subjects was used for evaluating the system performance using statistical procedures. Fifteen subjects were selected randomly to provide 20 genuine siguatures over a course of one month. Five subjects were selected randomly to provide one simple forgery for each of the 15 subjects given only the printed name of the person, and other five subjects provided skilled forgeries given sample of genuine signatures and allowed to practice, one for each of the 15 subjects. The FRR for the case of skilled forgeries is 3.0% and the FAR is 8%. For the case f simple forgeries, both the FRR and FAR rates are 0.0%.

In [14], a hybrid technique integrated both geometrical features with Multi Resolution Analysis (MRA) ased features. A vector quantization classifier and a neural network classifier were used to classify the ulti-resolution features. Features extracted at different scales proved more effective in image analysis. ecause signatures of the same person are likely to differ on one, but not on several scales. A database omprised 450 signatures that were collected from 25 people. An authentic signature database was built from 15 people. Five were asked to write a set of free-handed forgeries, and the other five were asked to produce a set of simulated forgeries of the 15 subjects. A total of 20 signatures were collected from each person. The training set includes 15 of the signatures and the remaining five are used for testing the system. The multi-resolution analysis used a cubic spline for the wavelet transformation and is performed on both the horizontal and vertical projections of the signatures until the length of the horizontal projection was 2 and the length of vertical projection was 4. The same MRA was performed on the signature image itself For signature classification, two classifiers were used: VQ classifier and a three-layer feed forward neural classifier. A neural network was built for each scale of the multi-resolution representation. The outputs of the elementary networks are grouped to form the output for an individual. The verification error rate of the VQ classifier scheme was 6.7% while that for the multi-resolution analysis was 4.9%.

In [15], the design and implementation of a signature processing system is reported. The signature verifier is based on a back propagation neural network approach. The system achieves a performance of up to 80%. The input to the neural network for verification consists of all the pixels that made up the signature image. The image is acquired by optical means and reduced to a standard size.

In [16], neural networks are used for signature verification to detect casual forgeries. Genuine signatures and forgeries were used for training neural networks. A database including 380 genuine signatures is collected over two years from five individuals. The same five individuals signed 265 forgeries in which the individuals knew the name of the person whose signature was being forged but had not viewed a genuine signature. Signatures were normalized to a size of 128 X 64 size. A FRR of 3% and FAR of zero-effort forgeries of 3% has been reported.

In [17], a statistical model is used for signature recognition and verification. The model involves an average signature (intrinsic shape function) which is independent of speed, location, scale and orientation The used signature base is constructed from 10 signatures from each writer. Results are not reported.

In [18], a comparative study is conducted for evaluating the performance of parametric and reference pattern based features in static signature verification. Reference pattern based features are extracted from both the horizontal and vertical projections Similar features are extracted from the unknown pattern. Other features such as slant, high density factor, and the normalized global base line are extracted. A signature database including 200 genuine is obtained from 20 subjects and 200 forgeries are skillfully simulated by 10 forgers Experimental investigations showed that the reference pattern based features significantly improved the verification system as the result of being independent of the signature position in the document.

In [19], a structural approach is described for signature description. Signature description involves two groups of structural and geometrical features:

(a) Global features such as
- the dominant slant
- if the signature has lower zone parts or not
- the number of elements in the signature
- ratios between signature length and width
- ratios between middle zone width and signature width

(2) Local features such as:
- slant as measured on the element
- the high density factor
- the comparison relation between the length of each element and its precedent, starting from left to right.
- The position relation between the element baseline and the global baseline.

Signatures are processed for removal of noise by performing the vertical projection of the signature extracted from background, finding the largest component in this projection and then eliminating all parts which does not belong to the largest component. The authors expect their approach to be effective in signature verification.

2.2 Device-based On-Line Approaches to Signature Recognition

Input devices in this category are either digitizing tables, or smart pens and hand gloves for the first time in this paper.

2.2.1 Digitizing Table - Based Systems

In [20], both global and local features that summarize aspects of signature shape and dynamics of signature production are used for signature verification with 3% equal error rate. Signatures are normalized for position, size, and orientation using the Fourier transform. The performance of the system is evaluated based on a test database consisting of 542 genuine signatures and 325 forgeries. Each reference set consisted of the first 6 signatures of every one of the 59 writers. A simple Euclidean distance classifier was trained on the first 6 signatures of the 59 writers and tested on 542 genuine signatures and 325 forgeries. The best false acceptance rate achieved is 7.5%.

In [21], the design of a FIR filter for on-line signature verification is discussed. The FIR is determined using the auto-correlation functions of both the horizontal and vertical velocities regarded as the input and output sequences of the filter. The horizontal and vertical velocities are calculated analytically by differentiating the normalized horizontal and vertical directions of the handwriting on a stroke of signature. The time duration of the signing is normalized to one. Experiments are performed on a database of one hundred Kanji signatures from six subjects. Type I error rates are found to be 2-12% while Type II error rates are found to be 0-2%.

In [22], an Autoregressive (AR) model is used in combination with a Hidden Markov Model (HMM) for writer identification. The signature, represented by a one dimensional spatial stochastic sequence, is decomposed into pseudo-stationary segments. Velocity, acceleration, and pressure profiles are not considered in this study. The evolution of abrupt and gradual changes in the contours is described by the AR-HMM. An AR-HMM is used to model each writer, the resulting model is a set of probabilities which can be used to calculate the overall probability of a particular observation sequence. A test signature is segmented, AR parameters are extracted for each segment, and these are quantized and assigned VQ code book values. A test writer signature is identified by comparing it to each of the writer models in the known writer population. The used training set includes 80 signatures from each of 16 writers, while the test set includes 20 siguatures. Another test set includes 70 signatures per writer. The classification results for 20 test siguatures are 97.5 % and 94.5% for the second set (70 signatures) with 95.1-98.7% confidence interval. The average FAR for the case of a single threshold in the first experiment is 4.375 and the average FRR is 4.375%.

In [23], a technique based on Bayesian Neural Network is presented for dynamic signature verificatioo of Chinese signatures. A set of 16 features is used: total time, average velocity, uumber of segments, average length in the eight directions of the signature, width/height ratio, left-part/right-part density ratio, and upper-part/lower-part density ratio. Experiments were performed on a database coosisting of 800 genuine signatures from 80 subjects and 200 simple and 200 skilled forgeries by 10 forgers. The FRR for the case of skilled forgers is abnut 2% FRR, and the FAR is 0.1% zero-effort.

In [24], a model in which a test siguature is assumed to consist of a reference signature which is transformed from occasion to occasiou is described. Five steps are used for signature verification. Signature data are recorded from a graphics tablet which recorded the (x,y) coordinates as well as the downward pressure on the pen. A cubic spline approximatiou is used to average out the measurement errors. Speed is computed from the smoothed signature. A time warp function is computed so that correspondence between

the reference signature and the signature being verified [illegible]. The signature is segmented using low speeds regions (low speed is 15% of mean speed) into a sequence of segments called letters. Finally, the reference signature is estimated by averaging. A distance measure is used for decision making.

2.2.2 Pen-based Systems

In [25], a system for on-line signature verification using LPC Cepstrum and Multi Layer Perceptron neural Networks is described. Cepstral linear prediction coefficients are extracted from the trajectories of signatures. A number of individual MLP networks receives the cepstral coefficients for training. The outputs of all neural networks is used for signature verification. A test database includes 321 genuine signatures from 27 subjects and 321 forgeries from two imitators is used for training the single output MLP's. The remaining 489 genuine signatures and 31 forgeries from another two imitators are used for obtaining the error rates. The genuineness of the input signatures from the test database is determined with an error rate of 4%.

In [26], an on-line signature verification system based on dynamic time-warpping (DWT) is described. The SmartPen is used to collect data such as pen-tip positions, speeds, accelerations or forces while a person is signing. Five pen signals are low-pass filtered with cut-off frequency 40 Hz. The resulting signals are sampled at 100 Hz. Dynamic time wrapping is used to deal with the presence of non-linear time differences between the test and reference signatures. Form and motion parameters are extracted as features. Signature classification is based on Mahalanobis decision making. Experiments are performed using 360 genuine signatures from 18 individuals, collected over a period of 3 months. For each writer 15 signatures are used as reference and the remaining signatures are used for testing. As forgeries for a certain person, the original signatures produced by the other signers are used. The optimal classification is achieved by using the Gabor transform-coefficients describing the signal content in the frequency range from 0 Hz to +/- 30 Hz. The Equal Error Rate (EER) is 1.5%. Another experiment is performed using the kernel approach for classification of form and motion features and achieved an EER of 0.3%. The authors note that the major drawback of their approach is that they use each of the 5 signals available individually, which neglects the link between signals.

In [27], a genetic algorithm based system is proposed for on-line signature verification. The invisible en-up parts of the signature are used to construct a signature verification system. Trajectories left in pen-up situation which are called "virtual strokes" are used to extract the optimal features which represent the personal characteristics of the authentic signature and affect the error rate greatly. Virtual strokes are used to extract 6 kinds of features to form the following candidate feature set:

1- length,
2- slope,
3- the biggest angle, it is the most acute angle in the part of curve
4- local curvature, and
5- the relative locations of the virtual strokes dis_x, and dis_y.

The Genetic Algorithm (GA) is used to select the most stable features from the candidate feature set. Signature verification is performed by applying a fuzzy network to the chromosomes in order to absorb the intrapersonal variability. Shapes of the fuzzy membership functions are determined using 5 randomly chosen signature from the signature database. Experiments are performed on 250 signatures (120 genuine signatures and 130 forgeries) acquired from 20 subjects. The rate of type I error is 6% and that of type II error is 0.8%.

In [28], a 4 layer back propagation neural network classifier is applied on pen pressure and speed of writing features which are extracted on-line from 70 persons signatures. The back-propagation network has an input layer of 768 neurons to which the pen pressure and the preprocessed speed are input. The output layer consists of one neuron and gives the degree of confirmation. A false rejection rate of 7.97% and an error ratio (False acceptance) of 0.61 % are reported. The system is constructed on a neuro-computer.

In [29], a comparative study is performed on signature verification from position, velocity, and acceleration signals. Three types of signal comparison algorithms are tested (dynamic time wrapping, regional correlation and [illegible]) on a signature database. The comparison shows that the most discriminant signals are signals which reflect vertical activity of the signing process and that the best representation space for 2D signature verification is the velocity domain. Signatures were digitized with a [illegible] tablet at a rate of 100 Hz and a resolution of 200 lines/inch. A database of 1950 signatures is collected from 59 volunteers. Data were acquired in 5 sessions, spaced one per day. No skilled forgeries were collected. For each signature, the database contains [illegible] signals: the pin tip position, the pin

tip velocity and the acceleration signals were computed from the position signals in two directions.

In [30], an automatic signature verification system that is based on data analysis and clustering methods is described. This approach uses geometric features such as number of connected components, number of loops, quantified cumulated phase for signatures on their whole, and initial direction of track pen coded in four quadrants together with dynamic features such as total duration, duration of connected components and mean and maximum velocities in connected components. Two experiments were performed . First, a new linear stepwise discriminant classifier (14 classes) was applied to the reference set. The classifier maximizes the ratio of between-class scatter to within-class scatter. A partition by hyper planes permitted 99.7% of valid classification on test-set elements then an iterative process for dynamic clustering was used.

2.2.3 Hybrid Apprnaches to Signature Recognition

In [31], 'Counter-match', Dynamic Signature Verification (DSV) using neural computing methods, offers a reliable means of confirming a person's identity without resorting to additional biometrics such as fingerprints or hand-prints. Counter-match is a DSV package which works with electronically captured signatures. The system compares both the shape of a signature and the speed of writing the signature. The neural network is embedded within an 'elastic' pattern matching code. Elastic pattern matching allows two shapes to be matched even though there are small differences between the shapes. The code is designed to be tolerant of natural variations in signatures - but critical of forgeries leading to a very robust verification system.

In [32], a signature base consisting of 6 consecutive lodgings was used as a reference set. A set of different features like frequency based features (Fourier spectrum) , geometrical features (length of signature) , and dynamic features (time, speed, pressure and acceleration) is used for signature verification. The reported recognition accuracy is about 95% and the error rate is 1/10,000. Optimization of a descriptive feature vector for each individual signer results in a system which adapts its behavior to the individual signature characteristics.

In [33], a transputer based system is implemented for signature verification. Experiments are performed on a database of 40 sample signatures from 24 subjects. The samples were divided to provide independent training and test sets. The system was able to perform correct verification with zero error. The used feature set is not reported.

2.2.4 Glove-based approaches to Signature Recognition

The Glove represents an easy to use device that can reflect the identity of a person and renders the forging process nearly impossible. The dynamic features of hand glove provide information on:

1- patterns distinctive to an individuals signature and hand size
2- time elapsed during the signing process
3- hand trajectory dependent rolling

To the authors best knowledge, hand gloves have never been used in the field of signature recognition. Gloves are used now for the first time in a signature recognition system. Wide application in banks and internet based applications could be enhanced by manufacturing light and wireless hand glove.

While most input devices offer one, two, or three degrees of freedom, the data glove is unique in that it offers multiple degrees of freedom for each finger and for the hand as well. This permits a user to communicate to the computer a far richer picture of his or her intentions than most other input devices. As digital information grows in quantity and importance in the workplace, more efficient means of manipulating it will increase in importance. However, this rich expressive power also brings added complexity to the input processing side of the system.

This research is an initial attempt to demonstrate the data glove as an effective high-bandwidth data entry device for signature recognition. We believe that the glove will be the most effective and secure device for developing a signature recognition system. We now look at the data glove and its signature recognition using the following precepts:

1. To improve system security
2. The signature recognition algorithm must assume a low performance/low cost glove. The average consumer will not spend exorbitant amounts of money on an input device, and the easiest way to cut the cost of today's data glove is to reduce its resolution. An example of such a glove is 5DT's data glove, which provides mid-range performance but whose cost is $500 (1997).
3. The signature recognition algorithm should not focus exclusively on the static position of the hand at any time, but also on the use of rate-of-change information.

Glove as a tool for signature recognition allows authentication of people not only through the biometric characteristics of their signature but also through the size of their hand. The virtual signature acquired by the glove can be used to make Internet transactions or bank transfers secure, because it unequivocally authenticates a person. In order to increase its user friendliness, gloves for this purpose must be wireless. The author believes that the Virtual Signature is the most reliable way for signature authentication specially when the signing process takes place on a digitizing table as well. This combination results in all possible useful features like finger and hand dynamics, speed, time, acceleration and the effect of hand size.

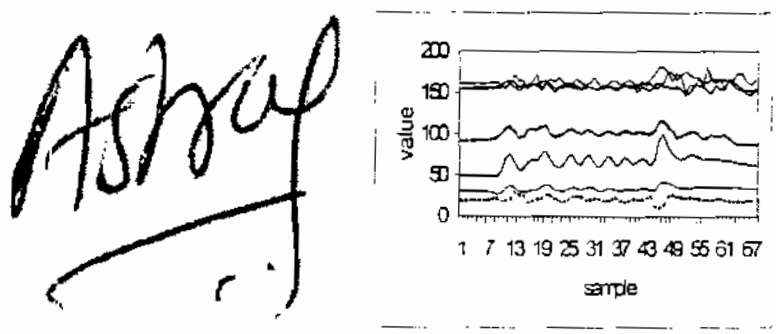

(a) (b)

Figure 2 (a) A typical signature on paper and the correspondiog seven glove signals

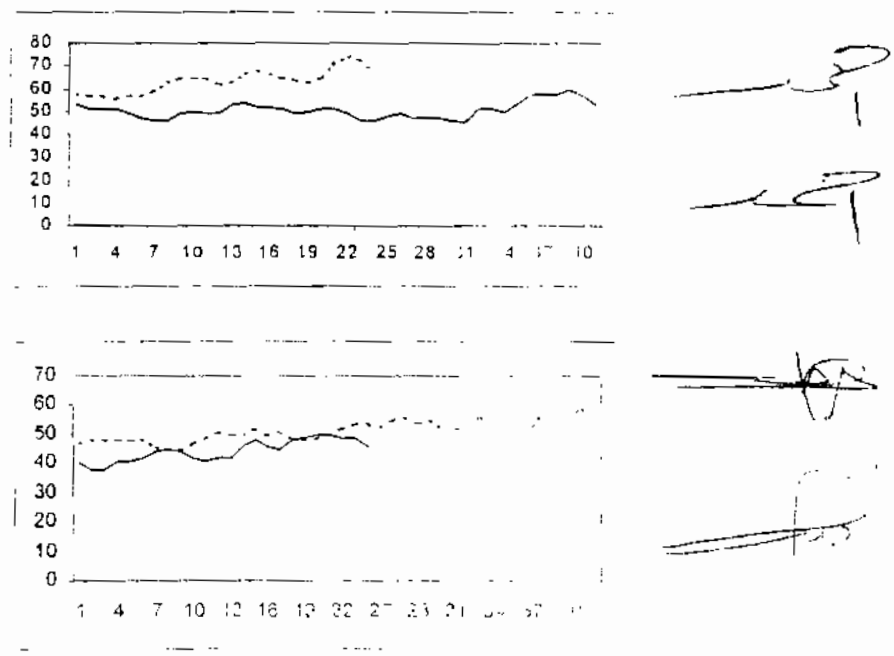

(b)

Figure 3a,b Signals of the thumb for original and forged signatures

The reliability of algorithms was tested with records from the standard AHA database, it has been found that the algorithm based on neural wavelet network can detect all the beats by learning under any condition without false positives, time advance or time delay, and it is faster than the neural network algorithms due to the use of the wavelet function.

Therefore, it can be concluded that the algorithm developed by Dickhaus H., Heinrich H (1996) and based on neural-wavelet-network is able to detect all beats regardless of its shape and it is the most insensitive algorithm to the different types of noise.

REFERENCES

1- Abou-chadi, F.E.Z., and saleh, M.M., "An Adaptive QRS Detection Algorithm With Variable Threshold," Mansoura Eng. Journal, vol. 17, No .2, pp. E1-E12, Dec (1992)

2- Afonso VX, Tompkins WJ, Nguyen TQ, Trautmanns, and Luo S., "Filter bank-based processing of the stress," ECG. Proc. Annu. Int Conf. IEEE Eng. Med. Biol Soc., Sep (1995).

3- Afonso, V. X., Tompkins, W. J., Nguyen, T.Q., Trautmann, S., and Luo, S., "Comparing Stress ECG Enhancement Algorithms," IEEE Engineering in Medicine and Biology Magazine, May/June (1996).

4- Ahlstrom, M.L., and Tompkins, W.J., "Digital Filters For Real-Time ECG Signals Processing Using Microprocessors," IEEE Trans. Biomed. Eng., vol. BME-32, pp. 708-713, Sep. (1985)

5- Beal, R. and Jackson., T. Neural Computing. (1990).

6- Balda, R. A. et al. The HP ECG Analysis Program Trends in computer-processed Electrocardiograms, J.H. Van Bemmel and J. L. Willems, Eds. North Holland. pp. 197-205, (1977).

7- Daubechies. Orthonormal bases of compactly supported wavelets. Pure Appl. Math., vol. 41, (1988).

8- Dickhaus H., Heinrich H. "Classifying Biosiguals with Wavelet Networks," IEEE Engineering in Medicine and Biology Magazine, (1996).

9- Engelese W.A.H. and Zeelenberg C., "A single scan algorithm for QRS-detection and feature extraction," IEEE comput. Card., Long Beach: IEEE Computer Society, pp. 37-42 (1979).

10- Fraden, J., and Neuman, M.R., "QRS Wave Detection," Med. Biol. Eng. Comput. vol. 18, (1980).

12- Friesen, G.M., Jannett, T.C., Jadallah, M.A., Yates, S.L., Quint, S.R., and Nagle, H.T., "A Comparison of The Nnise Sensiuvity of Nine QRS Detection Algorithms," IEEE Trans. Biomed. Eng., BME-37, pp. 85-98, Jan. (1990).

13- Gustafson, D., et. al. Automated VCG Interpretation studies using signal Analysis Techniques. R-1044 charles stark Draper Lab., Cambridge, MA, (1977).

14- Hamilton, P.S., and Tompkins, W.S., "Evaluation of QRS Detection Algorithms Using The IBM PC," Proc. of the IEEE/Seventh Annual Conference of the Eng. in Medicine and Biol. Society, (1985).

15- Holsinger, W.P., et al., "A QRS Preprocessor Based on Digital Differentiation," IEEE Trans. Biomed. Eng., vol. BME-18, pp. 212 -217, (1971).

16- Kohn, A. F., and Furuie, S.S., "Safety In Medical Signal Analysis," IEEE Eng. in Medicine and Biology Magazine, vol.BME-10, no. 4, pp. 56-62, Dec (1991).

17- Liu, C.S., Yu, B.C., Lee, M., Chen, J. J., and Chen, C.Y., "A Nonlinear Digital Filter For QRS-Complex Detection," IEEE/Seventh Annual Conf. of the Eng in Medicine and Biol. Soc., (1985).

18- Mahoudeaux, P. M. et. al., "Simple Microprocessor-Based System for On-Line ECG Analysis", Med. Biol. Eng. Comput., vol. 19, pp. 497-500. (1981).

19- Menard, A. et. al., "Dual Microprocessor System for Cardiovascular Data Acquisition. Processing and Recording," in Proc. IEEE Int. Conf. Industrial Elect. Contr. Instrument., PP. 64-69, (1981).

20- Okada, M., "A Digital Filter For The QRS Complex Detection," IEEE Trans. Biomed. Eng., vol. BME-26, pp. 700- 703, Dec (1979).

21- Pan, J., and Tompkins, W.J., "A Real-Time QRS Detection Algorithm results," IEEE Trans. Biomed. Eng., vol. BME-32, pp. 230- 236, Mar. (1985).

22- Qiuzhen Xue, Yu Hen Hu, and Tompkins.W. J. , "Neural-Network-Based Adaptive Matched Filtering for QRS Detection," IEEE Trans Biomed. Eng., vol,.BME-39, No. 4, April. (1992).

23- Ruha, A., Sallimen, S., and Nissilla. S.,"A real-rime microprocessor QRS detector system with 1-ms timing accurracy for the measurment of ambulatory HRV," IEEE Trans. Biomed. Eng. Vol. BME-44, PP.159-167, March (1997)

24- Saleh, M. M. Comparison of the noise sensitivity of QRS detection algorithms. MSc. Thesis, Mansoura University, (1993).

Algorithms based on linear and nonlinear filtering, (c) Algorithms based on neural networks, and (d) Algorithm based on wavelet transform and wavelet neural networks.

The detection timing accuracy and detection reliability of the selected algorithms were tested with two types of ECG databases: six tapes of the standard American Heart Association Database (AHA) and a synthesized normal ECG (used as a gold standard) corrupted with six types of simulated noise: (a) electromyographic interference (EMG), (b) powerline interference, (c) baseline drift due to respiration, (d) abrupt shifts in the baseline, (e) motion artifacts, and (f) a composite of the above noise types. This approach has been adopted to test the QRS detection performance of a real-time microprocessor system published recently (Ruha, et al. 1997). It provides a precise time reference to be used for comparison. This cannot be achieved with natural ECG recordings as the time reference is unknown. Also, the annotations in the AHA records cannot be used as time references as the time resolution in those records is low due to the low sampling frequency of 250 Hz used.

It has been found that algorithms based on digital differentiators give generally lower performance as the differentiation process has frequency characteristic that amplifies the signal and the noise occuring in the region between the highest ECG signal frequency components (here, 100 Hz) and the Nyquist frequency (in our case 125 Hz), thus increasing the algorithm efficiency.

Algorithms based on linear digital filtering give higher performance even under low signal-to noise ratios. However, these algorithms suffer from two problems: 1) the signal passband of the QRS complex is different for different subjects, 2) the noise and QRS complexes passbands overlap. Moreover, the linear phase characteristics of these filters do not cause phase distortion to the input signal, however, they cause certain time delay. This is clear from the detected time advance (TA) and time delay (TD) in the position of the detected QRS complexes. Algorithms based on nonlinear filtering give good results, algorithm D3, is able to discriminate between noise and QRS complexes, algorithm D4 give good results by using the length of the window suitable to the length of the QRS complex, a considerable time advance and time delay was obtained for these algorithms this is referred to the effect of the non-linear phase characteristics of each filter that affect the location of the QRS peak.

As for the algorithms based on neural network based adaptive matched filtering can model the inherently nonlinear ECG signal and detects all QRS complexes , however, it detects time delay and time advance.

The wavelet transform algorithm, can detect all QRS complexes in the precense of extreme noise but it detects false positives, as during transformation process, the R wave is transformed into more than one peak with high amplitude, and this algorithm has the advantage of saving memory and computation time.

Algorithms based on neural and wavelet network give the highest performance and the most accurate timing. They can detect all QRS complexes without time delay nor time advance. However, the wavelet network algorithm has the advantage of saving the computation time, as the features of the signal were extracted in the wavelet domain and were sent as input to the neural-network. For this reason it has half the learning time required for algorithm of multi-layer-forward neural-network.

The ability of the algorithm to detect all the QRS complexes without any false positives depends on the method for selecting the value of the scaling constant by performing a tuning procedure for each algorithm on each type of noise, while each algorithm has a maximum potential to discriminate between noise and the QRS, which depends on the optimum selection of parameters

Tape Number	Number of Beats	The detected beats	% detection
1201	1623	1298	80%
2202	2246	2066	92%
8204	2352	2187	93%
6206	2785	2701	97%
4207	2006	1965	98%
8209	2026	2026	100%

Tape Number	Number of Beats	The detected beats	% detection
1201	1623	1298	80%
2202	2246	2066	92%
8204	2352	2234	95%
6206	2785	2729	98%
4207	2006	1985	99%
8209	2026	2026	100%

Table-17 Results of application of Algorithm D3 to the AHA tapes.

Tape Number	Number of Beats	The detected beats	% detection
1201	1623	1363	84
2202	2246	2066	92
8204	2352	2234	95
6206	2785	2729	98
4207	2006	1965	99
8209	2026	2005	99

Table-18 Results of application of Algorithm D4 to the AHA tapes.

Tape Number	Number of Beats	The detected beats	% detection
1201	1623	1379	85%
2202	2246	2088	93%
8204	2352	2234	95%
6206	2785	2729	98%
4207	2006	1985	99%
8209	2026	2026	100%

Table-19 Results of application of Algorithm D5 to the AHA tapes.

The Tape Number	The number of Beats	The detected beats	The detected beats percentage
1201	1623	1509	93%
2202	2246	2133	95%
8204	2352	2282	97%
6206	2785	2729	98%
4207	2006	1965	98%
8209	2026	2005	99%

Table-20 Results of application of Algorithm N1 to the AHA tapes.

Tape Number	Number of Beats	The detected beats	% detection
1201	1623	1623	100%
2202	2246	2246	100%
8204	2352	2352	100%
6206	2785	2785	100%
4207	2006	2006	100%
8209	2026	2026	100%

Table-21 Results of application of Algorithm N2 to the AHA tapes.

Tape Number	Number of Beats	The detected beats	% detection
1201	1623	1460	90%
2202	2246	2133	95%
8204	2352	2234	95%
6206	2785	2729	98%
4207	2006	1985	99%
8209	2026	2005	99%

Table-22 Results of application of Algorithm W1 to the AHA tapes.

Tape Number	Number of Beats	The detected beats	% detection
1201	1623	1460	90%
2202	2246	2066	92%
8204	2352	2234	95%
6206	2785	2701	97%
4207	2006	1945	97%
8209	2026	2005	99%

Table-23 Results of application of Algorithm W2 to the AHA tapes.

Tape Number	Number of Beats	The detected beats	% detection
1201	1623	1623	100%
2202	2246	2246	100%
8204	2352	2352	100%
6206	2785	2785	100%
4207	2006	2006	100%
8209	2026	2026	100%

IX- Conclusion

This work has been concerned with automatic detection of QRS complexes. The main focus has been to compare the performance of the QRS detection algorithms under different circumstances of low signal-to-noise ratios. Advanced digital signal processing techniques are applied to investigate the timing accuracy and reliability of each algorithm and to find out why some QRS detection algorithms are more sensitive to certain type of noise than others. A detailed evaluation procedure was performed to identify the algorithm that possesses the highest performance in the presence of various types of interfering noise and at different noise levels.

Seventeen QRS detection algorithms were selected for this work, from a literature survey according to their simplicity and high performance. The selected algorithms were then classified into four basic types: (a) Algorithms based on digital differentiators, (b)

based on differentiators and digital filters lie between 94% and 98%, while those of algorithms based on neural networks and wavelet transform lie between 97% and 100%.

As for Tape 4207, the percentage of correct detection of algorithms based on differentiators and digital filters lie between 95% and 99%, while those of algorithms based on neural networks and wavelet transform lie between 97% and 100%.

Tape 8209 gives the best performance at all because it has R- wave with large amplitude than the T and P. The percentage of correct detection of all the algorithms lie between 99% and 100%.

It can be concluded that algorithms N1 and W2 can detect 100% of the QRS beats existing in each tape. However, Algorithm W2 has the advantage of consuming the computation time.

Table-7 Results of application of Algorithm A1 to the AHA tapes

Tape Number	Number of Beats	The detected beats	% detection
1201	1623	1054	65%
2202	2246	1909	85%
8204	2352	2187	93%
6206	2785	2701	97%
4207	2006	1965	98%
8209	2026	2026	100%

Table-8 Results of application of Algorithm A2 to the AHA tapes

Tape Number	Number of Beats	The detected beats	% detection
1201	1623	1136	70%
2202	2246	2066	92%
8204	2352	2234	95%
6206	2785	2729	98%
4207	2006	1985	99%
8209	2026	2026	100%

Table-9 Results of application of A3 to the AHA tapes.

Tape Number	Number of Beats	The detected beats	% detection
1201	1623	1071	66%
2202	2246	1909	85%
8204	2352	2187	93%
6206	2785	2701	97%
4207	2006	1965	98%
8209	2026	2026	100%

Table-10 Results of application of Algorithm A4 to the AHA tapes.

Tape Number	Number of Beats	The detected beats	% detection
1201	1623	1136	70%
2202	2246	1796	80%
8204	2352	2093	89%
6206	2785	2617	94%
4207	2006	1905	95%
8209	2026	2026	100%

Table-11 Results of application of Algorithm A5 to the AHA tapes.

Tape Number	Number of Beats	The detected beats	% detection
1201	1623	1071	66%
2202	2246	1819	81%
8204	2352	2187	93%
6206	2785	2645	95%
4207	2006	1965	99%
8209	2026	2026	100%

Table-12 Results of application of Algorithm A6 to the AHA tapes.

Tape Number	Number of Beats	The detected beats	% detection
1201	1623	1071	66%
2202	2246	1864	83%
8204	2352	2234	95%
6206	2785	2645	95%
4207	2006	1945	97%
8209	2026	2026	100%

Table-13 Results of application of Algorithm A7 to the AHA tapes.

Tape Number	Number of Beats	The detected beats	% detection
1201	1623	1054	65%
2202	2246	1796	80%
8204	2352	2187	93%
6206	2785	2645	95%
4207	2006	1945	97%
8209	2026	2026	100%

Table-14 Results of application of Algorithm A8 to the AHA tapes.

The Tape Number	The number of Beats	The detected beats	The detected beats percentage
1201	1623	1379	85%
2202	2246	1909	85%
8204	2352	2234	95%
6206	2785	2701	97%
4207	2006	1965	98%
8209	2026	2005	99%

Table-15 Results of application of Algorithm D1 to the AHA tapes.

Table-16 Results of application of Algorithm D2 to the AHA tapes.

6- Composite Noise

The results of applying the selected algorithms to the simulated ECG corrupted with composite noise are listed in Table-6. Composite noise can be considered as great challenge as EMG noise since six algorithms are not able to detect all beats, most of the algorithms detect false positives. Algorithms A1, A2, A3, A6 and A7 give the lowest performance Algorithm A4 detects 30 beats with 6 false positives. and, algorithm A5 was able to detect all beats with 4 false positives, 20 false negatives.

Algorithms based on linear and nonlinear filtering give good results, algorithm D1 was able to detect 30 beats with 16 ms time advance, algorithm D2 detects 30 beats with 4 ms time delay and 12 ms time advance. Algorithms D3 and D5 detects all beats with 1 beat false positive. Algorithm D4 detects all beats with 8 ms time advance.

Algorithm based on neural network based adptive matched filtering N2 detects 29 beats with 3 false positives. Algorithm W1 detect all beats with 10 beats false positives, 2 multiple detection and 48 ms time advance. Algorithms N1 and W2 can detect all beats without time advance nor time delay. They give the highest performance.

Table-5 The results of applying the 17 algorithms to ECG corrupted with motion artifact noise.

Algorithm	TP	FP	FN	TD	TA	MD	TP %
A1	30	0	30	1	10	0	100%
A2	25	8	24	0	7	2	93%
A3	30	0	24	0	4	1	100%
A4	30	0	26	2	5	0	100%
A5	30	0	40	0	10	0	100%
A6	20	5	100	2	5	0	66%
A7	30	0	11	0	5	0	100%
A8	30	2	34	0	11	0	100%
D1	30	5	40	0	9	0	100%
D2	29	0	40	2	6	0	96%
D3	29	2	53	0	8	0	96%
D4	30	1	31	0	5	0	100%
D6	30	0	20	10	0	0	100%
N1	30	0	58	0	0	0	100%
N2	29	4	19	3	2	0	96%
W1	30	2	58	0	4	1	100%
W2	30	0	58	0	0	0	100%

Table-6 The results of applying the 17 algorithms to ECG corrupted with composite noise.

Algorithm	TP	FP	FN	TD	TA	MD	TP %
A1	25	5	25	0	20	5	83%
A2	27	8	100	1	10	1	90%
A3	27	0	20	0	11	1	90%
A4	30	6	18	0	12	0	100%
A5	30	4	20	2	10	0	100%
A6	25	5	17	0	12	4	83%
A7	28	10	17	0	5	2	93%
A8	30	0	19	0	2	0	100%
D1	30	0	20	0	4	0	100%
D2	30	0	19	1	3	0	100%
D3	30	1	25	0	13	0	100%
D4	30	1	16	0	5	0	100%
D6	30	1	20	10	0	0	100%
N1	30	0	50	0	0	0	100%
N2	29	3	10	3	3	1	96%
W1	30	10	58	0	12	2	100%
W2	30	0	50	0	0	0	100%

VIII- Results of the AHA databases

The results of applying the 17 algorithms on six different AHA tapes are given in Tables 7-23. Since 60% of these tapes were obtained from inpatients, the tapes used in this study contain different cases of abnormalities and the data suffer from baseline wandering. The results obtained from Tape number 1201 are the worst, as it contains T wave with high amplitude and the S-T interval is missed. The percentage of correct detection of algorithms based on differentiators and digital filters lie between 65% and 93%, while those of algorithms based on neural networks and wavelet transform lie between 90% and 100%.

The results of Tape 2202 are better than tape 1201. It has T-wave with high amplitude in some beats, other beats have inverted T- waves. and the R- wave has different amplitude. The percentage of correct detection of algorithms based on differentiators and digital filters lie between 80% and 95%, while those of algorithms based on neural networks and wavelet transform lie beteen 92% and 100%.

The percentage of correct detection obtained from Tape 8204 using the algorithms based on differentiators and digital filters lie between 89% and 97%, while those of algorithms based on neural networks and wavelet transform lie between 97% and 100%. Tape 6206 gives also good results The percentage of correct detection of algorithms

and wavelet transform give the best results they can detect all beats without time advance nor time delay and it can be concluded that algorithms N1 and W2 are the best of all as they can detect all beats without time advance nor time delay. However, W2 has the advantage of saving the compuation time.

4- Abrupt Shift

The results obtained using the simulated ECG corrupted with abrupt shift are listed in Table-4. This type of noise is a slightly greater challenge than the baseline drift due to respiration. Algorithms A1, A3, A4, A5, A7 and A8 were able to detect all beats. Algorithm A2 give low performance as it detects only 70% of the total number of beats. Algorithm A6 is the worst, it detects only 40% of the total number of beats.

Algorithms based on linear and nonlinear filtering give good results, algorithms D1, D4, D5 were able to detect all beats and algorithms D2 and D3 detect 96% of the beats.

Algorithms N1 and N2 were able to detect all beats. Algorithms based on wavelet transform were able to detect all beats with one beat false positive, 30 beats false negatives, and 40 ms time advance.

It can be concluded that algorithms N1 and W2 give the highest performance. They can detect all beats without time advance nor time delay.

Table-3 The results of applying the 17 algorithms to ECG corrupted with base line drift noise due to respiration.

Algorithm	TP	FP	FN	TD	TA	MD	TP %
A1	28	10	90	0	10	0	93%
A2	26	0	50	0	5	0	86%
A3	27	0	53	2	2	0	90%
A4	30	0	30	0	0	0	100%
A5	30	0	20	1	2	0	100%
A6	30	0	40	15	0	0	100%
A7	30	0	15	2	2	0	100%
A8	30	0	30	0	10	0	100%
D1	30	0	44	0	0	0	100%
D2	30	0	46	1	0	0	100%
D3	30	0	40	0	20	0	100%
D4	30	0	44	0	30	0	100%
D5	30	0	20	10	0	0	100%
N1	30	0	58	0	0	0	100%
N2	30	0	90	2	3	0	100%
W1	30	2	52	0	10	0	100%
W2	30	2	98	0	3	0	100%

Table-4 The results of applying the 17 algorithms to ECG corrupted with abrupt shift noise.

Algorithm	TP	FP	FN	TD	TA	MD	TP %
A1	30	0	60	0	30	0	100%
A2	21	10	44	10	20	0	70%
A3	30	0	39	0	8	0	100%
A4	30	9	35	2	9	0	100%
A5	30	0	50	1	10	0	100%
A6	12	2	124	6	8	0	40%
A7	30	0	19	0	0	0	100%
A8	30	1	30	0	5	0	100%
D1	30	1	55	0	9	0	100%
D2	29	1	40	2	9	0	96%
D3	29	1	56	0	10	0	96%
D4	30	1	49	0	9	0	100%
D5	30	0	20	10	0	0	100%
N1	30	0	58	0	0	0	100%
N2	30	2	10	3	2	0	100%
W1	30	1	30	0	10	1	100%
W2	30	0	58	0	0	0	100%

5- Motion Artifact Noise

The results of applying the seventeen algorithms using the simulated ECG corrupted with motion artifact noise are listed in Table-5. Motion artifacts are much like base line drift due to respiration but having lower frequency and amplitude.

Algorithms A1, A3, A4, A5, A7 and A8 detect all the beats. However, algorithm A2 detects 25 beats with 8 beats false positives and 7 samples time advance, algorithm A6 detects only 20 beats. Algorithms based on linear and non-linear filtering give good results. Algorithms D1, D4 and D5 detect all beats. Algorithms D2 and D3 detect 29 beats. Algorithm N2 detects 29 beats with 10 false negatives, 4 false positives, 3 samples time delay and 2 samples time advance.

Algorithm W1 was able to detect all the beats with 2 false positive. Algorithms N1and W2 can detect all the beats without time advance nor time delay.

Algorithms based on linear and nonlinear filteriug are able to detect the QRS beats with a small number of false positives However, algorithms D2, D3, D4 are unable to locate all of the QRS complexes. It is possible that the QRS complexes are suppressed along with the noise by the filtering algorithms.

Algorithms based on neural network N1and N2 gave high performance without false positives nor time advance or time delay They detect all beats with a small number of false negatives. Algorithms based on wavelet transform can detect all the beats but with a large number of false positives. Algorithm W2 is the best of all. It detects all beats without time delay nor time advance since this type of algorithms has the ability to learn. Moreover, it has the advantage of saving the computation time

2- Power Line Interference

The results obtained from the seventeen algorithms using the simulated ECG corrupted with 50 Hz powerline interference are listed in Table-2. These results are considerably more better than those for the EMG interference. The frequency spectrum for the simulated powerline interference consists only of the 50 Hz fundamental component. Most of the algorithms gave good results. Algorithms A1, A2, A3, and A8 are able to detect all the QRS complexes with correct detection of 96%-100%.

Algorithms A4, A5, A6, and A7 give also the worst performance as in the case of EMG noise Algorithms based linear and nonlinear filtering give good results as they are able to detect all beats. As for algorithms based on neural networks. Algorithm N1 can detect all the beats without any false positives, time delay nor time advance. Algorithm N2 is able to detect all beats with 3 beats false positives.

Algorithm W1 can detect all beats with 60 beats false positives while algorithm W2 can detect all beats, without false positives nor time advance or time delay Therefore, algorithms N1 and W2 give the best performance. They can discriminate between 50 Hz noise and QRS complexes aud would always be preferable.

Table-1 The results of applying the 17algorithms to ECG corrupted with EMG noise

Algorithm	Tp	FP	FN	TD	TA	MD	Tp%
A1	29	9	144	2	17	2	96%
A2	30	0	146	2	30	0	100%
A3	29	6	144	3	7	0	96%
A4	26	22	124	3	17	2	86%
A5	25	25	118	2	6	3	83%
A6	27	27	123	0	17	1	90%
A7	26	30	124	0	7	1	86%
A8	30	15	102	0	7	3	100%
D1	30	5	118	0	1	1	96%
D2	27	1	137	3	1	2	90%
D3	27	10	97	0	2	0	90%
D4	29	8	105	0	2	0	96%
D6	30	5	124	10	1	1	93%
N1	30	0	58	0	3	0	100%
N2	29	3	120	3	5	2	96%
W1	30	60	58	0	0	0	100%
W2	30	1	58	0	9	1	97%

Table-2 The results of applying the 17 algorithms to ECG corrupted with power line interference

Algorithm	TP	FP	FN	TD	TA	MD	TP%
A1	29	9	144	2	7	0	96%
A2	30	0	201	1	9	0	100%
A3	29	6	201	1	9	0	96%
A4	27	22	124	3	9	0	90%
A5	28	25	121	1	9	0	93%
A6	28	27	123	0	5	1	93%
A7	27	30	122	0	1	1	90%
A8	30	15	102	0	5	0	100%
D1	30	5	80	0	5	0	100%
D2	30	0	136	3	3	0	100%
D3	29	8	150		5	0	96%
D4	30	5	150		5	0	100%
D6	0	0	0	0	0	0	0%
N1	30	0	58	0	0	0	100%
N2	30	3	58	3	5	0	100%
W1	30	60	58		5	0	100%
W2	30	1	58		5	0	100%

3- BaseLine Drift Noise Due to Respiration

The results obtained using the simulated ECG corrupted with baseline drift noise due to respiration are listed in Table-3 Baseline drift due to respiration presents a lesser challenge to all of the algorithms except those based on amplitude and first derivative All of the other algorithms give ideal performance Algorithms based on neural network

great deal of experimentation was used to determine the different constants and thresholds needed to detect the QRS complexes to get the best form of adaptation. A tuning procedure was carried out in order to determine the value for these constants.

V. The Software Structure

The software for the evaluation was written in C language and executed on an IBM-PENTIUM-MMX-CPU 200 MHz computer. It consists of five major components. The collection of algorithms and digitized ECG data files make up two of the components. A scoring algorithm and a routine to tabulate the results account for the additional blocks. The fifth part is amain program which integrates the four modules.

VI. The Evaluation Criteria

As for the synthesized ECG data, the exact location of the QRS complex is known before the noise sources are added, the scoring algorithm developed by Hamilton and Tompkins, (1985) compares the onset of the QRS candidate to a key array containing the locations of all of the valid QRS onset. If the candidate onset falls between the actual onset and the end of the QRS complex (a window of 22 sample points or 88 ms was chosen), it is scored as a true QRS detection (TP). If the candidate onset occurs outside these boundaries, and less than the end of the T wave (200 sample points or 800 ms following the actual onset), it is counted as a false positive (FP). If the candidate onset occurs outside of these boundaries, it is scored as a false negative (FN). The percentage of QRS complexes correctly detected is calculated at the end of each run by dividing the number of QRS complexes correctly detected by the total number of actual QRS complexes. Since the search for the next QRS complex resumes at the next point following the candidate onset, it is possible that the same QRS complex will be detected more than once. Only the first correct detection will be included in the scoring of QRS-complexes found or the measure of delay. Subsequent detections which fall within the boundaries of the first detected QRS were classified as multiple detection (MD).

An indication of the time delay (TD) and time advance (TA) are also calculated after each run. If the detection occurs before or after the actual onset but within the proposed window (22 sample points), it is classified as an advanced or a late detection, respectively. The number of sample points between the onset and the detection are summed for all of the detections of that run. As for the AHA data, the number of the QRS complexes detected was determined and then compared to the number of beats registered in the tape.

VII. Results of Simulated Database

1- Electromyographic Noise (EMG)

The results obtained from the application of the seventeen algorithms using the simulated ECG corrupted with EMG is listed in Table-1 (expressed in samples). This kind of noise represents the greatest challenge to the majority of algorithms as it possesses broad-band frequency characteristics which overlap the frequency spectrum of the QRS complex, the amplitude of the QRS is, however, considerably greater than the noise. Only seven algorithms were able to detect all the QRS complexes.

Algorithms A1, A2, A3 and A8 give high performance with a small number of false positives. Algorithms A4, A5, A6, A7 have the worst performance as EMG noise has first and second derivative characteristics that are similar to those of the QRS.

target patterns are updated by shifting the time window one step forward, and the weights of the model are updated by the generalized delta rule with the error propagated back-wards.

D- Algorithms Based on Wavelet Transform and Wavelet Neural Networks

Two algorithms based on the utilization of the wavelet transform and the wavelet neural networks are considered. These are denoted by W1 and W2.

Algorithm W1

The algorithm was developed by Daubechies, (1992). The input array *x(i)* represents the ECG datasamples of length *N* which is an integer of power 2. The wavelet transform is computed as

$$y(i) = C_0 * x(i) + C_1 * x(i+1) + C_2 * x(i+2) - C_3 * x(i+3) \qquad 0 < i < N-4$$
$$y(i+1) = C_3 * x(i) - C_2 * x(i+1) + C_1 * x(i+2) - C_0 * x(i+3) \qquad 0 < i < N-4$$
$$y(N-6) = C_2 * x(0) - C_3 * x(1) - C_0 * x(i-6) + C_1 * x(i-5) \qquad 0 < i < N-4$$
$$y(N-5) = C_1 * x(0) - C_0 * x(1) - C_3 * x(i-6) - C_2 * x(i-5) \qquad 0 < i < N-4$$

Search the waveform [*y(i)*] for the points which exceed a threshold value *M* given as $M = C$ Max [*y(i)*], where *C* is a constant less than unity. Then the QRS complex cadidate occurs when *y(i)* > M

Algorithm W2

This algorithm was developed by Dickhaus and Heinrich, (1996). It utilizes the well-known multi-layer perceptron [MLP].

A wavelet neural network N can be described as an expanded perceptron with so-called wavelet nodes as preproeessing units for feature extraction. The wavelet nodes, which are adjusted during the learning phase, are modified versions, $h((t-\tau_k).a_k)$, of a basis wavelet *h(t)*. The nodes are described by a shift parameter, τ_k, and a scale parameter, a_k, which is inversely related to the node's frequency. These parameters correspond to the variables of the wavelet transform Formally, the node's output, ϕ_{ik}, is defined as the inner product of the node h_k and the signal s_i, which is the wavelet net's input (the index $i = 1, \ldots, N$ denotes the signal number)

During the training phase, the least-square error, $E = \sum_{i=1}^{N} \sum_{j=1}^{n} (d_{ij} - Y_{ij})^2 = min$

between the net's desired output vector, d_i, and its actual output, Y_i, again has to be minimized using, for example, a gradient technique Thus the wavelet parameters are varied to reduce the error E in each iteration, using a gradient technique. This procedure is repeated until the net has settled down to a minimum The complex Morlet wavelet has been chosen as the basis wavelet.

IV. Determination of the Algorithm Parameters

Each algorithm in this study is based on a specific scheme presented in the literature. However, they are not copies and should be considered as a [illegible] of the fundamental concept Each of them employed one or more [illegible] either as multipliers or as thresholds In some cases these constants were given in the literature, while in others they were not compatible with the [illegible] that we used. A

output of the nonlinear whitening filter is a linear combination of the outputs of the hidden units:

$$y_o = y_t - \hat{y}$$

$$y_t - \sum_{i=1}^{q} u_i z_{t-i} = y_t - \sum_{i=1}^{q} u_i f\left(\sum_{j=1}^{M} w_{ij} y_{t-j} - b_j\right)$$

The generalized delta rule is used to update the weights in the hidden layer. The least-mean-square error of this filter is

$$e = E\left\{\left(y_t - \sum_{i=1}^{q} u_i f\left(\sum_{j=1}^{M} w_{ij} y_{t-j} + b_j\right)\right)^2\right\}$$

The hidden layer weights are updated using

$$w_{t+1}^j = w_t^j + 2\mu\delta_j x_t + \alpha\left(w_t^j - w_{t-1}^j\right) \qquad j = 1, \ldots, q$$

where $w_t^j = \left(w_{1j}, w_{2j}, \ldots, w_{mj}\right)^T$ is the weight vector connected from the input units to the j th hidden unit; $\delta_j = yh_t^j\left(1 - yh_t^j\right)u_j e$ is the error term passed back from the upper layer; α is the step size of a momentum term.

The second step is to select a template, and then to filter it using a whitening filter. Then, a neural-network-based recognition method is used to update the template dynamically. The neural network model used is a three-layer feedforward back-propagation model, which has a number of inputs to cover the QRS complex. After the learning process is finished, the neural network coefficients are stored for determining a new template during the processing. Four recognized normal QRS complexes are kept in the template bank, and the newest template is the average of these four complexes, i.e.

$$QRS = \frac{1}{4}\sum_{i=1}^{4} QRS_i(i)$$

The corresponding most-recently-recognized QRS complex of the original signal is sent to the neural network recognition model. The model determines if the new QRS complex is one which should be put into the template bank. The template was filtered by the adaptive whitening filter synchronously with the filtering of the input signal. The whitened QRS template is

$$WQRS(i)_k = QRS(i)_k - \sum_{i=1}^{q} u_i f\left(\sum_{j=1}^{M} w_{ij} QRS(i)_{k-j} + b_j\right) \qquad k = 1, \ldots, L - M$$

where L is the length of the QRS template vector; and M is the number of input units in the model.

After both the whitened signal and the whitened template have been obtained, matched filtering is performed. The output of the matched filter is

$$y(t) = \sum_{i=1}^{L} WQRS_i y_w(t-i)$$

where WQRS is the whitened template and $y_w(t)$ is the output of the whitening filter of the original signal. The input ECG signals first go through an adaptive whitening filter having as a key part the neural-net-based nonlinear adaptive noise removal filter. The input layer of the neural net model gets the data vector from the ECG signal. In this case, the input pattern is the data vector $y(t-1) = \left\{y_{t-q}, y_{t-q+1}, \ldots, y_{t-1}\right\}^T$ and the target pattern is y_t. The output of the model is the estimation of y. In each epoch, the input and

time and frequency dependent processed version of the input signal, in which noise has been reduced without distorting ECG components of interest.

Let $X(n)$ represents the input ECG signal, then the filter output is $Y(n)$. Then,

$$Y(n) = \sum_{k=-7}^{7} C_{k-7} X(n-k) \qquad M \le n \le N-M$$

Searching across each 250 sample of Y(N) about the point which exceeds a threshold Q. Then QRS candidate occur *If* $Y(n) \ge Q$

C- Algorithms Based on Neural Networks

Two algorithms based on the utilization of neural networks are considered. These are denoted by N1 and N2.

Algorithm N1

This algorithm developed by Beal R., and Jackson T , (1990). The learning rule is the back propagation rule. The first step is to initialise weights and thresholds. Then all weights w_i and threshold are set to small random values The actual output of each layer is calculated

$$y_{pj} = f\left[\sum_{i=0}^{n-1} w_i x_i\right]$$

and passes that as input to the next layer, the final layer outputs values o_{pj}

Adapt weights starting from the output layer, and move backwards, using the equation

$$w_{ij}(t+1) = w_{ij}(t) - \eta \delta_{pj} o_{pj}$$

where $w_{ij}(t)$ represents the weights from node i to node j at time t, η, is a gain term, δ_{pj} is an error term for pattern P on node j

where $\delta_{pj} = k\, o_{pj}(1-o_{pj})(t_{pj}-o_{pj})$ for output units

and $\delta_{pj} = k\, o_{pj}(1-o_{pj})\sum_{k} \delta_{pk} w_{jk}$ for hidden units

Where the sum is over the k nodes in the layer above node j.

Algorithm N2

This algorithm was developed hy Qiuzhen XUE, et al (1992) It is based on a neural-network-based nonlinear adaptive filter. It involves the addition of a nonlinear hidden layer consisting of a number of nonlinear processing units Each of the hidden units produces a nonlinear intermediate result

$$z_i = f\left(\sum_{j=1}^{M} w_{ij} y_{(-j)} - b_j\right)$$

where $f(\ )$ is a sigmoid function defined as $f(x) = \dfrac{1}{1+e^{-\frac{x}{T}}}$

where T, is the temperature that controls the nonlinearity of the function The w_{ij}'s are the weights which the input units to the hidden units, and the b_j's are the bias terms. The

$$y_3(n)=[y_2(nT)]^2 \qquad 1 < n < N$$

Then a moving-window integration is used to obtain waveform feature information in addition to slope of the R wave. It is calculated from:

$$y_4(n)=\left(\frac{1}{M}\right)[y_3(n-(M-1))+y_3(n-(M-2))+\ .\ +y_3(n)]$$

where M is the number of samples in the width of the integration window.

Two thresholds I1 and I2 are automatically adjusted to float over the noise. This are computed from:

Signal peak *SPKI = 0.125 PEAKI + 0.875 SPKI* (if PEAKI is the signal peak)
Noise peak *NPKI = 0.125 PEAKI + 0.875 NPKI* (if PEAKI is the noise peak)
THRESHOLD I1 = NPKI + 0.25 (SPKI - NPKI) and THRESHOLD I2 =0.5 THRESHOLD I 1

The signal peak SPKI is a peak that the algorithm has already established to be a QRS complex. The noise peak NPKI is any peak that is not related to the QRS (e.g., the *T* wave). The thresholds are based upon running estimates of SPKI and NPKI. When a new peak is detected, it must first be classified as a noise peak or a signal peak. To be a signal peak, the peak must exceed THRESHOLD I1 as the signal is first analyzed or THRESHOLD I2 if search back is required.

Algorithm D4

Chung-Shyan Liu et al., (1985) developed an algorithm utilizes the median filter. The input signal *X(n)* is filtered by a median filter of window size 5 (i.e, $M = 2$) followed by a Hanning filter. Let the outputs of the median filter and Hanning window be denoted by Y(n) and Y(n) respectively, then

$$Y_0(n)=median[X(n-2),...,X(n-1),X(n),X(n+1),\ .\ ,X(n+2)] \qquad 2 < n < N\text{-}2$$

$$Y_1(n)=\frac{1}{4}Y_0(n-1)+\frac{1}{2}Y_0(n)+\frac{1}{4}Y_0(n+1) \qquad 1 < n < N-1$$

A second median filter of window size $2M + 1 = 7$ to $Y_1(n)$. The QRS-complexes will be smeared out. However, other components of the ECG, P-waves, T-waves, and baseline wander will be reserved. Now, we denote the output by $Y_2(n)$

$$Y_2(n)=median\ [Y_1(n-M),\ .\ ,Y_1(n-1),Y_1(n),Y_1(n+1),\ .\ ,Y_1(n+M)] \quad M < n < N-M$$

To remove baseline drifts, compute the difference between $Y_1(n)$ and $Y_2(n)$ as:

$$Y_3(n)=Y_1(n)-Y_2(n) \qquad M < n < N-M$$

A QRS complex candidate occurs when a point in *Y(n)* exceeds a threshold value calculated from $TH = C\ .\ max\ [Y_3(n)]$

Algorithm D5

Afonso V.X., et al. (1995, 1996) developed an algorithm based on filter bank (FB). The algorithm decomposes the ECG into *32* uniform subband frequencies of the signal. The 0 to 180 Hz frequency bandwidth of the input signal is decomposed into 32 uniform frequency subbands, *{[0 to 5.625], [5.625 to 11.25],.....[174.375 to 180]}Hz.*

The subband in the [0 to 5.625] Hz range, which contains most of the energy of the P and T waves, is not processed in any way. In the remaining subbands, the signal components are attenuated to various levels in time periods that correspond to the non QRS region. The QRS region of the ECG is not modified in any of the subbands. The processed subband signals are then reconstructed by the synthesis filters to result in a

The squared differences between $Y_0(n)$ and $Y_1(n)$ was computed as .

$$Y_2(n) = [Y_1(n) - Y_1(n)]^2 \qquad m < n < N - m$$

The data points $Y_2(n)$ are the output from the band-pass filter which form peaks at locations where the spikes exist in $[Y_0(n)]$

The next step is to compute the modified waveform $Y_3(n)$ as:

$$Y_3(n) = Y_2(n) \left[\sum_{k=n-m}^{n-m} Y_2(k) \right]^2 \qquad m < n < N - m$$

Then a rectification procedure is carried out. A weight is placed on $Y(n)$ as follows

$$Y_4(n) = k \; . \; Y_2(n) \qquad m < n < N - m$$

where $k = 1$ if $[Y_0(n) - Y_0(n - m)] \; . \; [Y_0(n) - Y_0(n + m)] > 0$

$k = 0$ otherwise

Then a QRS candidate occurs when $Y_4(n) > h$ where h is an arbitrary threshold.

Algorithm D2

This algorithm was developed by (Engelese and Zeelenberg 1979). The ECG is passed through a differentiator with a 62 5 Hz notch filter

$$Y_1(n) = X(n) - X(n-1) \qquad 1 < n < N-1$$

The differentiated, filtered data is then passed through a digital low-pass filter.

$$Y_2(n) = Y_0(n) + 4Y_0(n-1) + 6Y_0(n-2) + 4Y_0(n-3) + Y_0(n-4) \qquad 3 < n < N-1$$

The output of the low-pass filter is scanned until a point with amplitude greater than a positive threshold is reached, i.e. if $Y_2(i) > PS$

If no other threshold crossing occurs within the 160 ms search region, the occurrence is classified as a baseline shift, otherwise, the following three conditions are tested

condition 1. if $Y_2(i + j) < NS \qquad 0 < j < 40$

condition 2. if $Y_2(i + j) < NS \quad 0 < j < 40$ and $Y_2(i + k) < PS \quad j < k < 40$

condition 3 if $Y_2(i + j) < NS \quad 0 < j < 40$ and $Y_2(i + k) > PS \quad 0 < k < 40$

and $Y_2(i + l) < NS \qquad k < l < 40$

If any of the above conditions apply, the occurrence is classified as a QRS candidate

Algorithm D3

This algorithm was developed by Pan and Tompkins, (1985) The difference equation of the low-pass filter is

$$y(n) = 2y(n-1) - y(n-2) + x(n) - 2x(n-6) + x(n-12) \qquad 12 < n < N$$

The difference equation of the low-pass filter is

$$y(n) = 32y(n-16) - [y(n-1) + y(n) - y(n-32)] \qquad 32 \quad n \quad N$$

A five-point derivative is then calculated

$$y_2(n) = \left(\frac{1}{8}\right)[-y(n-2) - 2y(n-1) + 2y(n+1) + y(n+2)] \quad 2 \qquad n < N-2$$

After differentiation, the signal is squared point by point, i.e

$$y_2(n) = ABS[\, x(n+2) - 2x(n) + x(n-2)\,] \qquad 1 < n < N-2$$

The rectified, smoothed first derivative is added to the rectified second derivative :

$$y_3(n) = y_1(n) + y_2(n) \qquad 2 < n < N-2$$

The maximum value of this array is determined and scaled to serve as primary and secondary empirical thresholds k_1 and k_2 respectively

$$k_1 \text{ (primary threshold)} = c_1 \,.\, max\,[\, y_3(n)\,] \qquad 2 < n < N-2$$

$$k_2 \text{ (secondary threshold)} = c_2 \,.\, max\,[\, y_3(n)\,] \qquad 2 < n < N-2$$

where c_1 and c_2 are scaling factors

The array of the summed first and second derivatives is scanned until a point exceeds k_1. A QRS candidate occurs when the next six consecutive points must all meet or exceed the secondary threshold k_2. i.e.

$$Y_3(i) > k_1 \qquad \text{and} \qquad Y_3(i+1),\ Y_3(i+2), \ldots\ldots Y_3(i+6) \geq k_2$$

Algorithm A8

This algorithm was developed by Abou-Chadi and Saleh, (1992). It calculates three statistical parameters of the ECG signal for a moving window of length N = 25 samples centered at the *kth* sample. These are:

Mean value $\overline{X_k} = \frac{1}{N} \sum_{i=k-m}^{k+m} X_i$, Standard deviation $\sigma_k = \sqrt{\frac{1}{N} \sum_{i=k-m}^{k+m} \left(\overline{X_i} - \overline{X_k}\right)^2}$

Third moment $M_k = \left[\frac{1}{N} \sum_{i=k-m}^{k+m} \left(\overline{X_i} - \overline{X_k}\right)^3 \right]^{\frac{1}{3}}$ *where* $N = 2m + 1$

A threshold value T_k is calculated for each sample using the formula:

$$T_k = C_1 \overline{X}_k + C_2 \sigma_k + C_3 M_k$$

where C_1, C_2, and C_3 are constants to be determined empirically

The difference Y_i between two successive samples $X(i)$ and $X(i+1)$ is formed, such that $Y(n) = X(n+1) - X(n)$. A QRS candidate occurs when a point X_k in X_i exceeds the threshold T_k and the corresponding time derivatives Y_k and Y_{k+1} change their sign

B- Algorithms Based on Linear and Nonlinear Filtering

Five algorithms based on the utilization of linear and nonlinear filtering techniques are considered. These are denoted by D1- D5.

Algorithm D1

This algorithm was developed by Okada, (1979) The first step, is to smooth the ECG data using a three point moving average filter.

$$Y_0(n) = [\, X(n-1) + 2X(n) + X(n+1)\,] / 4 \qquad 1 < n < N-1$$

The output of the moving average filter is passed through a low-pass filter. Let $Y_1(n)$ denote the output from the low-pass filter

$$Y_1(n) = \frac{1}{2m+1} \sum_{k=n-m}^{n+m} Y_0(k) \qquad m \quad n \quad N-m$$

points which exceed the negative (descending slope) threshold *(ns)*. All data points in the ECG between the onset of the rising slope and before the end of the descending slope must meet or exceed the amplitude threshold, i.e.

$y(i)\ ,\ y(i+1)\ ,\ y(i+2) > ps$ and $y(j)\ ,\ y(j-1) \le ns$

where $(i+2) < j < (i-M)$, and M is the number of samples of 100-ms duration depending on the sampling rate, and $x(i)\ ,\ x(i+1)\ ,\ \ldots\ ,\ x(j+1) \ge A$

Algorithm A4

Holsinger et al. (1971) developed a QRS detection scheme. The algorithm is based on the determination of the first derivative from the raw ECG data. The first derivative $Y(n)$ is calculated for the ECG using equation

$$Y(n) = X(n) - X(n-1) \qquad 1 < n < N$$

A QRS candidate is happened if $Y(n) > K1$ and a number of consecutive candidates (J) should be existed as follows.

$Y(i)$, $Y(i+1)$, $Y(i+2)$, *and* $Y(i-J) > K2$ where $K2$ is a constant threshold.

Algorithm A5

This algorithm was developed by Menard, (1981). The first derivative is calculated for each point of the ECG, using the formula.

$$y(n) = -2x(n-2) - x(n-1) - x(n+1) + 2x(n-2) \qquad 2 < n < N-2$$

A slope threshold (S) is calculated as a fraction (k) of the maximum slope for the first derivative array.

$$S = k.\ max\,[\,y(n)\,] \qquad 2 < n < N-2$$

The first derivative array was searched for points which exceed the slope threshold. The first point that exceeds the slope threshold is taken as the onset of a QRS candidate, i.e. $y(i) > slope\ threshold\ (S)$

Algorithm A6

This algorithm is a simplification of the QRS detection scheme presented by Balda, (1977). The absolute value of the first and second derivative are calculated from the ECG data. These are denoted by $y_0(n)$ and $y_1(n)$, respectively

$$y_0(n) = ABS[\,x(n+1) - x(n-1)\,] \qquad 1 < n < N-1$$

$$y_1(n) = ABS[\,x(n+2) - 2x(n) + x(n-2)\,] \qquad 2 < n < N-2$$

The two arrays $y_0(n)$ and $y_1(n)$ are scaled and then summed

$$y_2(n) = Ay_0(n) + By_1(n) \qquad 2 < n < N-2$$

where A and B are constants greater than unity

This array is scanned until an empirical threshold C is met, i.e. $y_2(n) \ge C$. Once this occurs, the next eight samples are compared to the threshold. If five or more of these eight points meet or exceed the threshold, a QRS candidate exists.

Algorithm A7

This technique was developed by Ahlstrom and Tompkins, (1985). The rectified first derivative is calculated from the ECG data

$$y_0(n) = ABS[\,x(n+1) - x(n-1)\,] \qquad 1 < n < N-1$$

The rectified first derivative is then smoothed using a Hanning filter

$$y_1(n) = [\,y_0(n-1) + 2y_0(n) + y_0(n+1)\,] \qquad 1 < n < N-1$$

The rectified second derivative is calculated

III. The Selected QRS Detection Algorithms

A large number of QRS detection schemes are described in the literature. It would be impractical to describe all of QRS detection algorithms because of their large numbers. Several considerations were used to limit the number of QRS detection schemes to reasonable cross section of the different basic techniques described. Only relatively simple and newly developed algorithms were selected. A convenient way for classifying the QRS detection algorithms has been adopted in this study as follows: (1)Algorithms based on the use of digital differentiators, (2) Algorithms based on linear and non-linear filtering, (3) Algorithms based on neural networks, and (4) Algorithms based on wavelet transform and wavelet neural networks.

A- Algorithms Based on Digital Differentiators

Eight QRS detection algorithms are based on numerical differentiation, either first- or second-order. These are denoted by A1-A8

Algorithm A1

The concept for this algorithm was taken from Gustafson, (1977). Let $X(n) = X(0), X(1),..., X(N)$ represent a one-dimensional array of sample points of the digitized ECG. The first derivative $Y(n)$ is calculated as.

$$Y(n) = X(n-1) - X(n-1) \qquad o < n < N-1$$

The first derivative is then searched for points which exceed a constant threshold C i.e $y(i) \geq C$ and the next three derivative values: $y(i-1), y(i+2)$ *and* $y(i+3)$ must also exceed C. If the above conditions are met, point X(*i*) can be considered as a QRS candidate if the next two sample points have positive slope amplitude products, i.e

$[y(i+1) . x(i-1)]$ *and* $[y(i+2) . x(i+2)] \geq 0.$

Algorithm A2

This algorithm was developed by Fraden and Neuman, (1980). A threshold (A) is calculated as a fraction *(k)*of the peak value of the ECG.

$$A = k . max [x(n)] \qquad 0 < n < N$$

The raw data is then rectified to remove the negative signal values as follows :

$y_{0(n)} = x(n)$ if $x(n) \geq 0$ and $y_0(n) = -x(n)$ if $x(n) < 0$ $\qquad 0 < n < N$

The rectified ECG is passed through a low level clipper

$y_1(n) = y_0(n)$ if $y_0(n) \geq A$ and $y_1(n) = A$ if $y_0(n) < A$

The first derivative is calculated at eaeh point of the elipped, reetified array .

$y_2(n) = y_1(n+1) - y_1(n-1) \qquad 0 < n < N$

A QRS occurs when a point in $y_2(n)$ exceeds a constant threshold C, i.e. $y_2(i) > C$.

Algorithm A3

This algorithm was developed by Moriet-Mahaudeaux, (1981). An amplitude threshold *(A)* is calculated as a fraction *(k)* of the largest positive valued element of the array of the ECG samples for instance: $A = k \max [x(n)] \qquad 0 < n < N$

The first derivative y(n) is calculated at each point of x*(n)* such that :

$$y(n) = x(n+1) - x(n-1) \qquad 0 < n < N-1$$

A QRS complex occurs when three consecutive points in *y(n)* array exceed a positive slope threshold *(ps)* and followed within the next *100 ms* by two consecutive

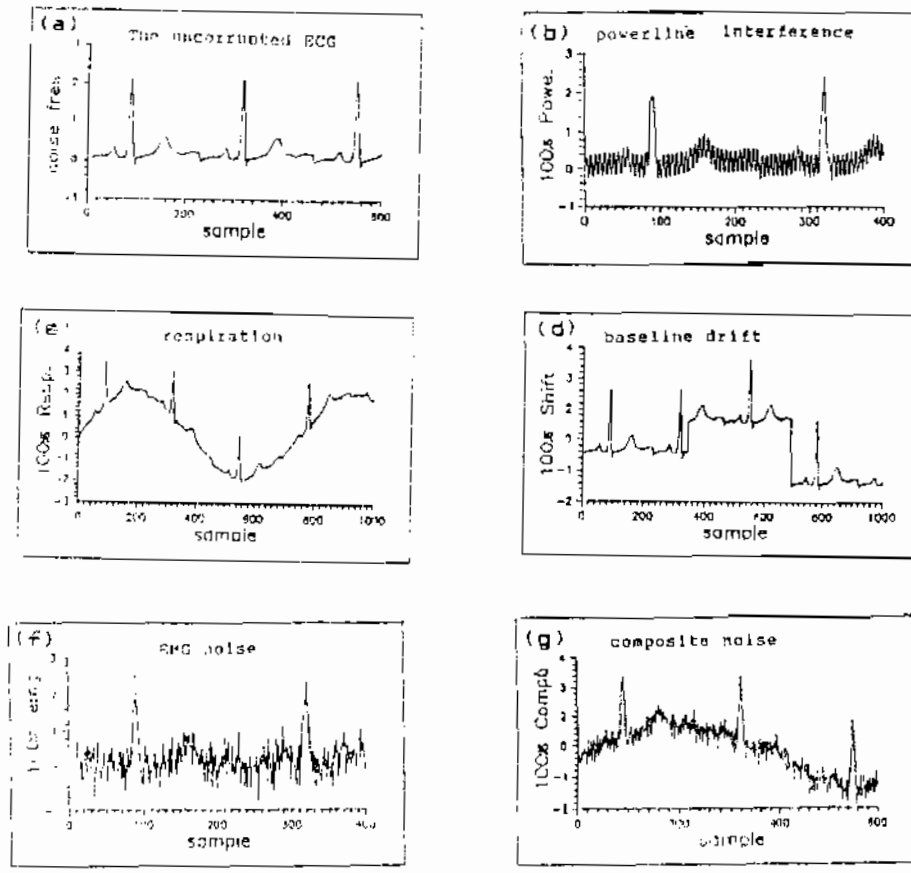

Fig 1 Synthesized ECG signal contaminated with different types of noise (a) The uncorrupted ECG signal (b)the signal corrupted with powerline interference, (c) with baseline drift due to respiration, (d) with abrupt shifts, (e) with electromyographic interference, and (f) with a composite of all noise

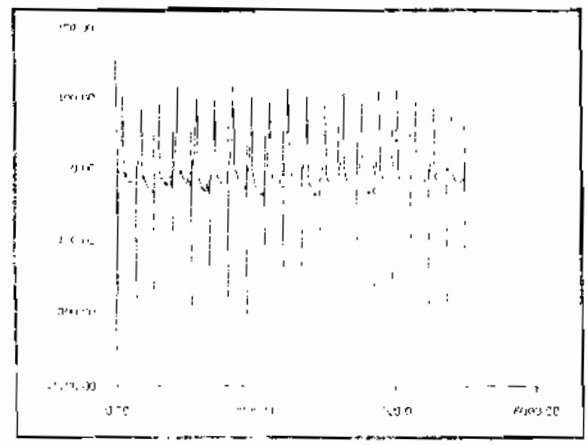

Fig (2) An exciting [illegible] of The MIT Database

I. Introduction

Automated analysis of electrocardiograms (ECG) is well established for use in: real time ECG monitoring in hospital intensive-care units and operating rooms, Holter-tape analysis, arrhythmia monitors, and high-speed processing of long-term ambulatory ECG recordings. QRS detection is the most important part in automated ECG signal analysis systems. After the QRS complex has been identified, the heart rate may be calculated, the ST-segment may be examined for evidence of ischemia, or the waveform may be classified as normal or abnormal. Thus a reliable QRS recognition algorithm is an important part of any ECG instrument.

QRS detection is a difficult task, not only because of the physiological variability of the QRS complexes, but also because of the various types of noise that can be present in the ECG signal. Noise sources include muscle noise, artifacts due to electrode motion, power-line interference, baseline wander and T-waves with high-frequency characteristics similar to QRS complexes. Most of the existing ECG analysis programs require a relatively noise-free digitized ECG; data corrupted with noise must either be filtered or discarded. However, filtering and other signal processing techniques can alter the signal and may result in the loss of clinically significant data: the processed signal may be distorted by the filter itself in such a way that their interpretation leads to a wrong diagnosis or an inadequate decision (Kohn, 1991). These issues are important design consideration for applications in real-time heart monitoring.

Previous studies reported by Friesen et al., (1990), and Saleh, M.M. (1993), quantify the relative noise susceptibility of several QRS detection algorithms However, in the past five years, a number of QRS algorithms have been developed. These algorithms are based on modern signal processing techniques such as: filter-bank, neural networks, wavelet transforms and wavelet neural networks. Therefore, it is required to study and compare the performance of these new algorithms in order to determine the algorithm that gives the best performance under different conditions of abnormalities

The main objective of the present work is to investigate the performance of seventeen QRS algorithms. These algorithms were chosen from the literature and are characterized by their high performance. The work also presents a general scheme to be followed for evaluating the performance of the QRS detection algorithms using two databases: a gold standard synthesized ECG contaminated with six types of noise as a first step of evaluation, and the standard American Heart Association Database (AHA).

II. Material

In order to evaluate the performance of the QRS detection algorithms we used two types of ECG database. (1) A synthesized normal ECG (used as a gold standard ECG) corrupted with five types of noise (Fig 1) These noise types were also combined to form a sixth composite noise source Consequently, the exact locations of the QRS are known before the noise source is added. This approach was developed by Friesen et al., (1990) for comparing the noise sensitivity of QRS detection algorithms. It allows accurate measurement of the ability of the algorithm to detect QRS complexes and to locate the onset of each complex in noise-corrupted ECG as well as in the noise-free ECG. The level of each type of noise was chosen to simulate the worst case that can be met in true records. (2) Six selected tapes of the Standard American Heart Association Database (AHA). Fig 2 shows an example of an AHA record